VELOCITY MEASUREMENTS AND FLOW STRUCTURE VISUALIZATIONS OF A SELF-SUSTAINED OSCILLATING JET

by

Dejan CVETINOVIĆ, Munenori UKAI,
Kazuyoshi NAKABE, and Kenjiro SUZUKI

The purpose of this study is the experimental investigation on self-sustained oscillating jet characteristics. Main aim was to describe vortical structures of turbulent air jet issuing from the nozzle of special configuration, modified by the controlled oscillations in free jet setup. In the present experiments was used so-called "whistler nozzle", a simple-structured device capable to induce self-sustained excitations with controllable frequencies depending on the nozzle geometrical configuration. The frequency of the excitation measured with a far-field condenser microphone probe was around 1-2 kHz. The jet Reynolds number was in the range 48,000-95,000 in all experimental conditions presented in this paper. Flow field velocity measurements were provided in the free jet setup, with and without self-sustained excitations. The images of both free and impinging jets were taken with a high-speed digital video camera. The flow field and structure of the jet were found to be extremely sensitive to the excitation and dependent on the excitation conditions. This fact can lead to the conclusion that the local heat transfer characteristics of jet impingement are also remarkably dependent on the jet excitation.

Key words: *self-sustained oscillation, whistler nozzle, impinging jet, velocity measurement, flow structure visualization*

Introduction

Impinging jets are used in a wide variety of industrial and technological applications such as gas turbine or electronic components cooling, drying of paper, textiles and film materials, and tempering of glass, due to high heat transfer rates obtained in a jet stagnation region. Hill and Greene [1] made experiments, in the first place, on jet-mixing rate of an interesting device that they named as "whistler nozzle". Acoustically modified jets, however, as a means of increasing entrainment was not a new idea even at this time. Crow and Champagne [2] successfully generated discrete frequency sound waves with a loudspeaker located upstream of their plenum chamber. By taking advantage of plenum chamber resonances, they were able to produce exit plane sinusoidal fluctuations in velocity up to 5% of the core velocity at specific frequencies. It has been shown by Hill and Greene that the whistler nozzle has produced the velocity fluctuations as high as 15%,

and more significantly, such fluctuations were produced without any external input. They studied this phenomena in the limited ranges of the parameters which directly influence the flow characteristics, but unsuccessfully obtained no correlations among the parameters. Hasan and Hussain [3] extracted from their more extensive data and showed the correlation between the whistler nozzle geometric parameters and the produced excitation frequencies. They've concluded that self-excited axisymmetric jets with pipe nozzles clearly have exciting possibilities, especially for controlling or modifying near-field transport phenomena including mixing of heat, mass, and momentum, entrainment, and aerodynamic noise generation. From a viewpoint of acoustical control of the jet, the whistler nozzle presents itself an attractive possibility because of its simple configuration, no requirement of external power, and ability to induce self-sustained oscillations of controllable amplitudes and frequencies over wide ranges.

In the present study, much attention was paid to experimental investigation of the velocity field of the turbulent air jet acoustically modified by the self-sustained oscillations in the whistler nozzle operation together with it's visualization with a high-speed digital camera.

Experimental apparatus setup and measurement techniques

Experimental apparatus

The experiments have been carried out in a laboratory with the precise control of air temperature and humidity. Figure 1 shows schema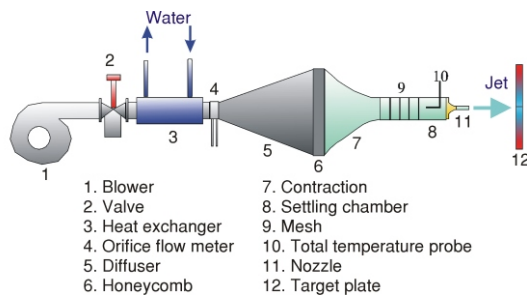tic view of the air-jet flow facilities with circular jet configuration, consisting of a blower, a valve, a heat exchanger, an orifice-type flow rate meter, a 10° diffuser, a honeycomb, a contraction, a settling chamber, and the whistler nozzle attached to the convergent nozzle at the end of the settling chamber. The settling chamber assures the axisymmetry of the flow upstream of the whistler nozzle. Several mesh screens are mounted inside the jet facility to reduce turbulence at the nozzle exit.

1. Blower	7. Contraction
2. Valve	8. Settling chamber
3. Heat exchanger	9. Mesh
4. Orifice flow meter	10. Total temperature probe
5. Diffuser	11. Nozzle
6. Honeycomb	12. Target plate

Figure 1. experimental setup

Experimental techniques

Velocity measurements were performed using a commercially-available I-type hot-wire probe. All probes used in experiments had the wire with the diameter and the

length 4 µm and 1.4 mm, respectively. The probe was operated as hot-wire velocity sensor by a constant-temperature module of the anemometer. The probe was mounted on a very accurate computer controlled 2-D traversing device, with the smallest step in both directions of 5 µm, for precise positioning inside the velocity field. Sampling rate was kept constant at level of 10,000 samples per second for all investigated cases, and for each measuring point were collected 10 sets of the one-second sequential digital data. After the data acquisition all signals were time-averaged and the appropriate velocity fluctuation and turbulence intensity were calculated.

The total temperature of the jet was monitored at position 10 in fig. 1 using an our-own made probe of a thin-thickness stainless-steel tube (1.4 mm I. D.) in which a K-type thermocouple pair was installed. The monitoring location was on the centerline of the settling chamber approximately 300 mm upstream of the whistler nozzle. The difference between the jet total temperature and the ambient temperature was carefully controlled within 0.1 °C in all experimental conditions, to avoid this temperature difference influence on the jet structure, which is especially important in the heat transfer experiments.

Acoustic measurements were carried out using a miniature far-field condenser microphone probe connected to an FFT analyzer.

The flow visualization system used to study the effect of acoustic excitation on the vortical structure of a jet was composed of a smoke generator, a continuous-wave Argon-ion laser with suitable set of lenses to obtain a desired thin laser sheet and a high-speed video camera connected to a computerized image capturing system.

Whistler nozzle configuration and operational characteristics

The device consists of a round tailpipe attached to the downstream end of a convergent jet nozzle and an axisymmetric collar sliding over the tail pipe, as shown in fig. 2. As a collar is pulled downstream a loud pure tone abruptly generates. This is called the first stage of the acoustic excitation. With increasing L_c, the tone increases in amplitude, reaches maximum, decreases and then disappears. With a further increase in L_c, the tone regenerates. This is the second stage, and so on. The tone frequency depends on the pipe-nozzle length L_p, the collar length L_c, the step height h (*i. e.* the difference between the inner radii of the nozzle and the collar), the nozzle diameter D, and the jet exit velocity U_e [3].
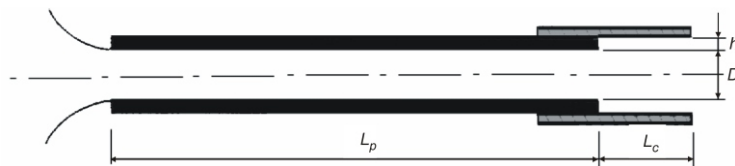

Figure 2. Experimental configuration: pipe-collar (whistler nozzle)

Flow characteristics of excited and non-excited jets

High speed camera visualization

Jet visualizations with the high-speed digital camera were performed to reveal the effects of self-sustained acoustic excitation on the vortical structures of the jet. Special attention was focused to the large-scale coherent structures in the incipient and transitional regions of the jet development. Visualized images of the jet flows actually revealed that acoustical perturbations could have remarkable influence on the short-length region from the nozzle lip and produce augmentation as well as suppression of turbulent velocity fluctuations depending on the jet Reynolds number, initial flow conditions and excitation Strouhal number [4]. Large augmentations of velocity fluctuation are associated with vortex pairing in the jet.

Initial shear layer instability near the nozzle lip results in a vorticity migration to form periodic, axisymmetrical coherent concentrations and leads to the laminar shear layer rolling-up to form periodic streaks of ring-shaped vortices [5]. The ring vortices convected downstream with growth in size undergo vortex-pairings with preceding or following vortices owing to the presence of a feedback loop mechanism, the loop of which is established between the nozzle exit and the location of vortex pairing [6]. In the late-transition region, the ring vortices are distorted owing to wave instability of their own cores, and collapse into large scale eddies. According to [7], the development of free jet is accompanied by the transition of an axisymmetrically coherent vortical structure to a less coherent turbulent structure with large scale eddies in the shear layer.

Figures 3, 4, and 5 show the set of high-speed video images taken at speed of 4,500 frames/s. The time difference between each images was 0.2 ms. The jet was seeded with smoke under the jet Reynolds number of 91,000 in a non-excited case ($St_e = 0$, fig. 3), an excited case ($St_e = 0.29$, fig. 4), and another excited case ($St_e = 0.52$, fig. 5). The flow direction of the jet, on all presented images, is from the right to the left side, and the stream-wise frame length of the captured image is approximately 3.5D. High-speed video
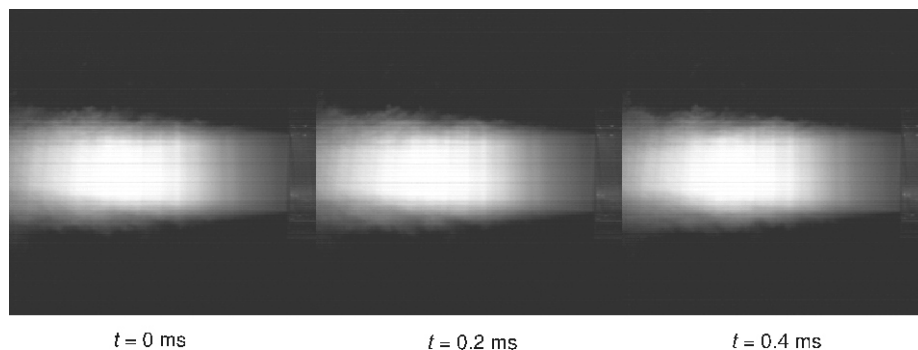

$t = 0$ ms $t = 0.2$ ms $t = 0.4$ ms

Figure 3. High-speed video images of non-excited jet, $L_p = 6D$; Re = 91,000

images of the non-excited jet in fig. 3, show small-scale non-organized vortical structures in the peripheral region of the jet, but no apparent structures in the potential core region. In the excited jet cases, on the other hand, the large-scale structures of vortex formation were clearly observed. Visualized scales of the vortical structure were found to be much larger in the case of $St_e = 0.29$ (fig. 4) than in the case of $St_e = 0.52$ (fig. 5). Also, the apparent length of the potential core appears to be shorter in the case of $St_e = 0.29$ than $St_e = = 0.52$. The condition of $St_e = 0.29$ corresponds close to the case of "preferred mode" ($St_e = 0.3$) according to [2] and [3].

Vortices convected downstream from the nozzle lip were observed to induce the periodical oscillations of the potential core. This is consequence of the fact that the large scale vortical structures, grown in size, can be found even at the jet axis at very short distance from the nozzle lip. The region near the nozzle lip in the excited case, in particular, of $St_e = 0.29$ close to the preferred mode, was observed to be very similar in structure to a
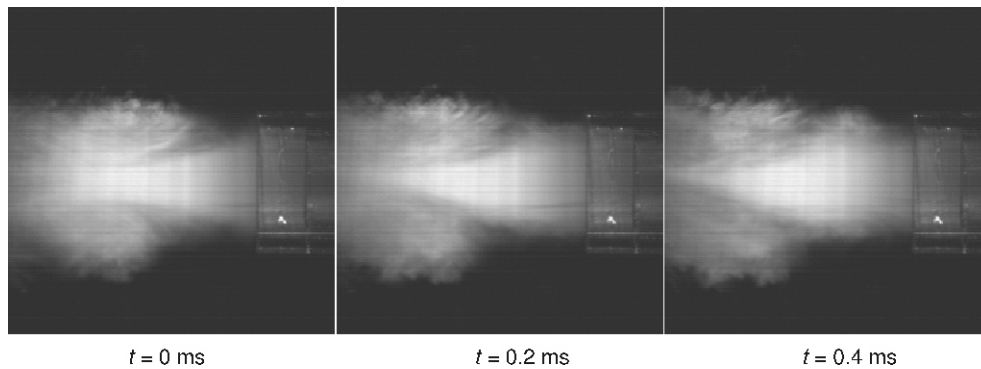

$t = 0$ ms $t = 0.2$ ms $t = 0.4$ ms

Figure 4. High-speed video images of excited jet, $St_e = 0.29$; $L_p = 6D$; Re = 91,000

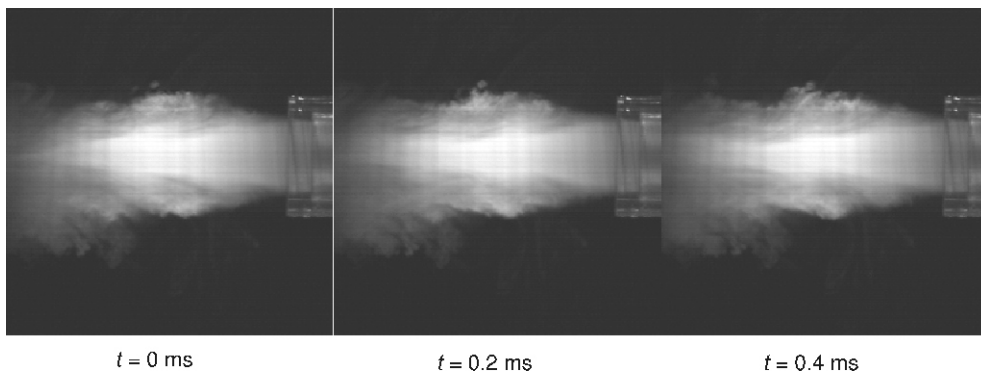$t = 0$ ms $t = 0.2$ ms $t = 0.4$ ms

Figure 5. High-speed video images of excited jet, $St_e = 0.52$; $L_p = 3D$; Re = 91,000

117

far downstream region of the non-excited jet. Excitation frequency close to the preferred mode could be effective in shortening the length of the potential core and increasing turbulent fluctuations in a shorter axial distance from the nozzle lip.

Jet excitation has remarkable influence on the region close to the nozzle lip and, for investigated sinusoidal excitations produced with the whistler nozzle of the given geometry, produces augmentation of turbulent velocity fluctuations depending on the Strouhal number and Reynolds number. Jet showed very high sensitivity to the excitation frequency, for further details see ref. [8].

Velocity and turbulence intensity

Velocity measurements were performed under the various conditions of nozzle geometry, flow rate and excitation frequency summarized in tab. 1. Main aim was to describe vortical structures of turbulent air jet issuing from the whistler nozzle, modified by the controlled oscillations in free jet. For these purposes, several sets of pipe nozzle with different lengths and the constant diameter, $D = 18$ mm, were manufactured. The step hight of the whistler nozzle was fixed at $h = D/8$, while the flow characteristics are varied in the range of Reynolds number 48,000-95,000 which corresponds to velocity range 40-90 m/s. The excitation Strouhal number, St_e, was varied in the range of $0.2 < St_e < 0.9$.

Table 1. Geometrical and flow experimental characteristics

Nozzle diameter, D [mm]	Nozzle length, L_p	Reynolds number, Re [–]	Nozzle exit velocity, U_e [m/s]	Excitation Strouhal number, St_e [–]
18	$3D$, $6D$, $9D$, $12D$	48,000-95,000	40-90	0.2-0.9

The results are presented as the axial distributions of time-averaged centerline velocity and turbulence intensity grouped by excitation Strouhal number. The axial distance from the nozzle exit, L, is measured from the end of the pipe nozzle along the jet axis in downstream direction, not depending on the collar position during the experiments with self-sustained excitation.

As mentioned before, the nozzle does not need any external power for producing oscillations in the jet. There was only one possibility to change the excitation Strouhal number – by changing jet velocity at the nozzle exit, due to the fact that for the fixed pipe length, the whistler nozzle could produce only fixed frequency and with the change of jet velocity only excitation amplitude was changed. The aim was to compare excitation cases with similar St_e to explore if the excitation Strouhal number is relevant parameter for the jet controlled excitation characterization. The experiments including the supply of external source for jet excitation can serve as relevant comparison [9].

The axial distributions of normalized time-averaged velocity against the normalized axial distance from the nozzle, grouped by Strouhal number, are shown in figs. 6, 7, and 8.
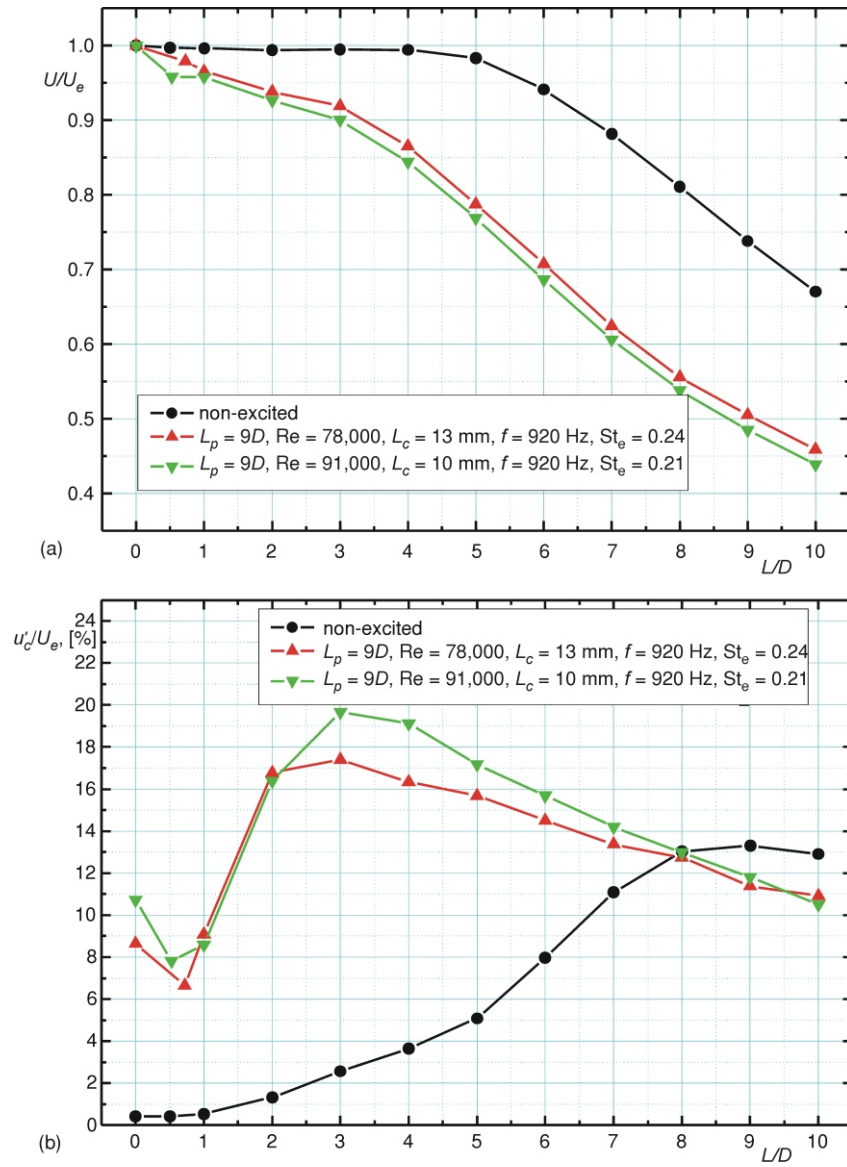

Figure 6. Axial distributions of:
*(a) normalized time averaged centerline velocity,
(b) turbulent intensity of non-excited and excited jet grouped by $St_e < 0.3$*
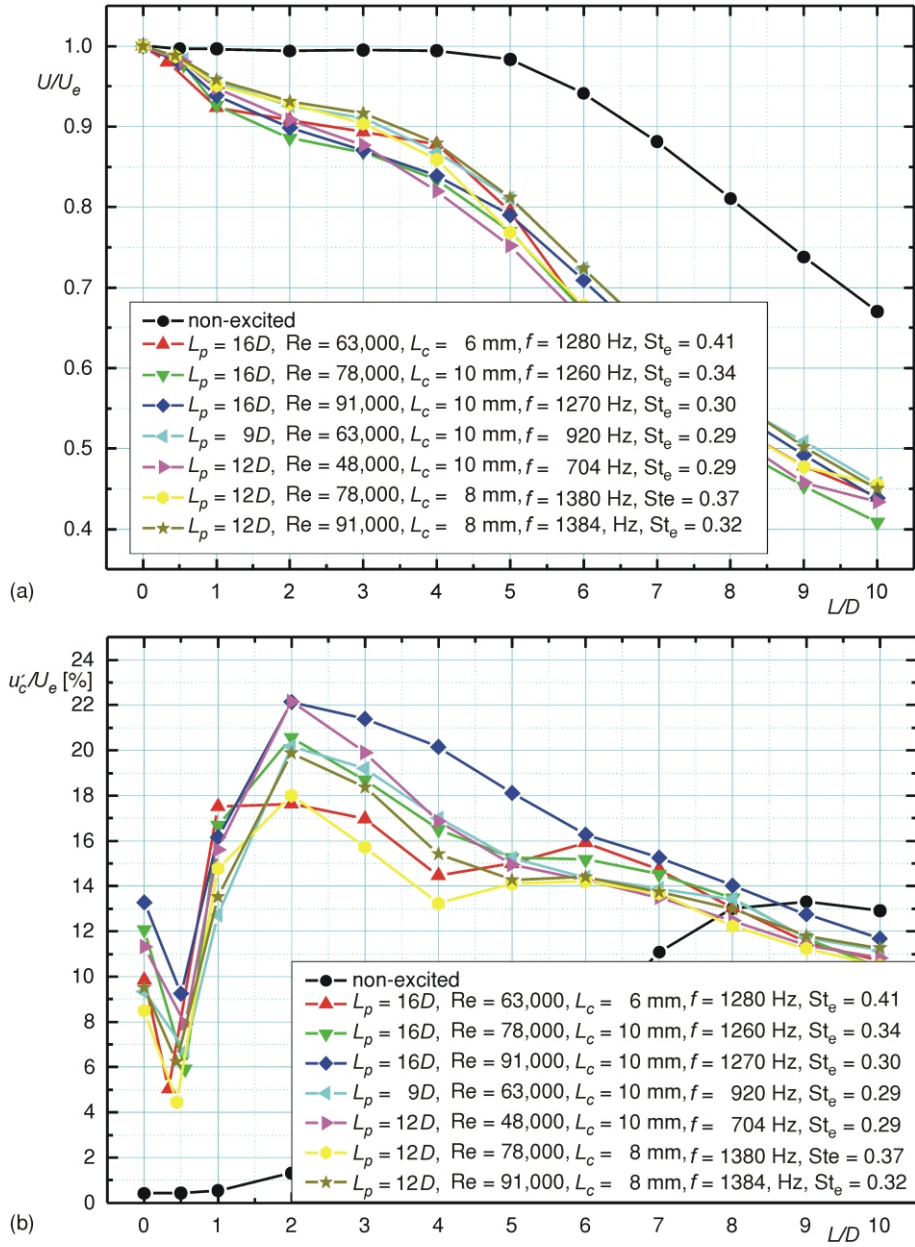
Figure 7. Axial distributions of:
(a) normalized time averaged centerline velocity,
(b) turbulent intensity of non-excited and excited jet grouped by $St_e \approx 0.3$-0.4
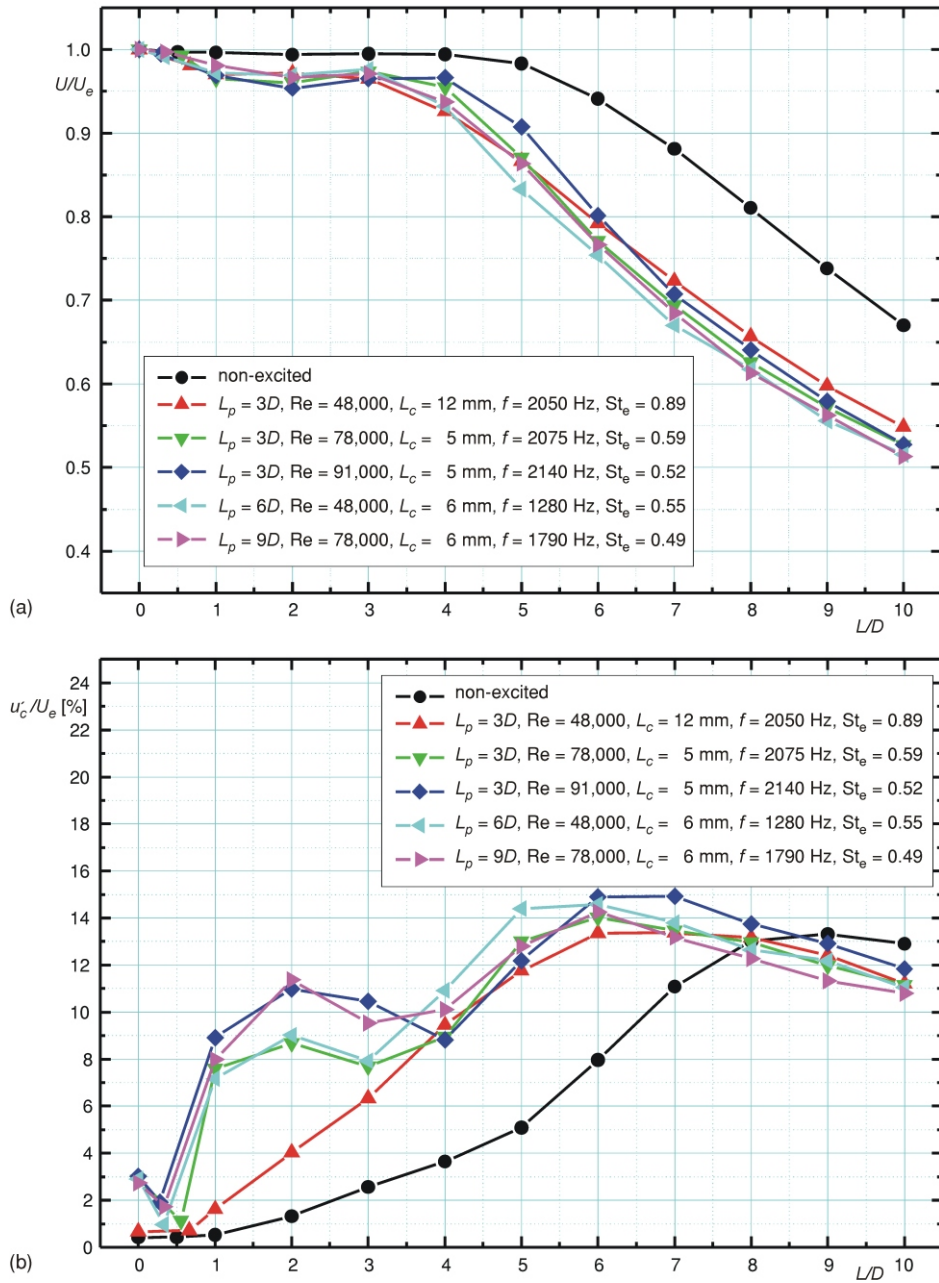
Figure 8. Axial distributions of:
(a) normalized time averaged centerline velocity,
(b) turbulent intensity of non-excited and excited jet grouped by $St_e >\sim 0.4$

Normalized time-averaged velocity profiles of non-excited turbulent jet show ordinary characteristics of the jets issuing from the circular nozzles. Normalized center-line velocity remains almost equal to the value measured at the nozzle exit up to normal-ized axial distance $L/D = 4$, followed with downstream deceleration of the jet velocity in larger axial distances. It is apparently clear that the measured normalized velocity pro-files have the potential core with constant jet velocity up to normalized axial distance be-tween 4 and 5.

Normalized time-averaged velocity profiles of excited turbulent jet show decel-eration of the jet velocity in all self-sustained excitation cases presented in this paper in comparison with non-excited turbulent jet velocity profiles. After sudden deceleration at the normalized axial distance equal to 1, in normalized velocity profiles, the flat areas with almost constant velocity could be found in the region from the nozzle exit to some axial distance depending on the excitation Strouhal number. This can lead to the conclu-sion that jet potential core still exists in the excited jet, but its length remarkably shortens depending on the excitation frequency.

Turbulence intensity of non-excited cases shows the characteristic distribution of the jet issuing from the circular nozzle. After low level of 0.4% at the nozzle exit, the turbulence intensity monotonically rises along the axial distance from the nozzle exit and reaches its maximum at distance of 9 nozzle diameters. Further decrease of the turbulence intensity is evident along the larger axial distances from the nozzle exit due to significant deceleration of the jet velocity. From the heat transfer point of view, the peak position of turbulence intensity distribution closely corresponds to the maximum in the Nuselt num-ber distribution.

Turbulence intensity profiles of all excited cases are clearly found to have a peak around $L/D = 2$-3, in comparison with the non-excited jet case, depending on the excita-tion Strouhal number. In the presented profiles it is obvious that initial excitation ampli-tude varies from case to case, due to the nature of self-sustained excitations that can be produced by the whistler nozzle, and also due to the limitations in varying the experimen-tal Strouhal number already explained in this paper.

Turbulence intensity profiles of the excitation cases of the Strouhal number close to 0.3, most amplified mode of excitation, show higher values of turbulence inten-sity compared to the other excitation cases. It can be clearly seen in fig. 7 that excitation amplitudes measured at the nozzle exit were in the range 10 to 14% for experimental Strouhal number of 0.3. Very high turbulence intensity values achieved in the experiment are probably derived from the applied turbulence intensity calculated without removing of the sinusoidal fluctuation component from the directly measured instantaneous veloc-ity composed of the following equation U $\overline{u}$ $\widetilde{u}$ u.

The peak position of maximum turbulence intensity profiles shifts close to the nozzle exit, which corresponds to the velocity decreasing on smaller axial distances from the nozzle lip comparing to the non-excited cases. Axial distributions of turbulence inten-sity show maximum values at axial distance of 2-3 nozzle diameters for excitation cases of Strouhal number close to $St_e = 0.3$-0.4, shown in fig. 7, while in the excitation cases $St_e < 0.3$, shown in fig. 6, and $St_e > \sim 0.5$, shown in fig. 8, axial positions of the maximum turbulence intensities are 3-4 nozzle diameters and 6-7 nozzle diameters, respectively.

122

At larger axial distances, the turbulent intensity values measured in these experiments (L/D = 9 and 10) are almost equal to those measured in non-excited jet. The excitation does not have any influences on the velocity profiles at higher axial distances from the nozzle lip. Transition into the small turbulent structures was already finished, and slight decreased values of turbulent intensity in this area are due to significant deceleration of the mean jet velocity, as already mentioned in the paper.

Significant decrease of the jet averaged velocity and the corresponding increase of turbulence intensity, at smaller axial distances from the nozzle, can lead to the conclusion that maximal heat transfer can occur in near-field of the jet compared to the non-excited cases, if the impinging plate is positioned perpendicularly to the jet flow direction.

Even if there was a significant difference in Reynolds numbers and geometrical parameters set in the present experiments, it is clearly shown that excitation cases can be grouped by excitation Strouhal number.

Conclusions

The present paper shows the results of experimental investigation of axisymmetric turbulent air jet characteristics modified by self-sustained oscillations in the whistler nozzle operation, which was visualized with the high-speed digital video camera and monitored using the hot-wire anemometry.

Visualization of the excited and non-excited air jets showed very high sensitivity of jet flow patterns to the excitation frequency. The excitation case close to the excitation Strouhal number of St_e = 0.3 produced a large-scale vortical structure in the regions nearer the nozzle lip than the other excitation cases. Also, the apparent length of the potential core becomes shorter in the case close to the preferred mode with St_e = 0.3.

Velocity measurement of excited jet cases showed evidence of the faster jet spread and decay at larger axial distances from the nozzle lip compared to non-excited jet cases for all the investigated excitation conditions.

All presented excitation cases can be clearly grouped by excitation Strouhal number, despite significant difference in geometrical and flow characteristics.

Excitation frequency with Strouhal number St_e = 0.3, close to the preferred mode, could be effective in shortening the length of the potential core and increasing turbulent fluctuations in a shorter axial distance from the nozzle lip.

Significant decrease of the jet time-averaged velocity and the corresponding increase of turbulence intensity at smaller axial distances from the nozzle can lead to the conclusion that the maximum heat transfer in impinging jet configuration can be obtained at shorter nozzle-to-plate distances compared to non-excited turbulent jet case.

Acknowledgment

Nomenclature

D – nozzle diameter, [mm]
f_e – excitation frequency, [Hz]
h – step height, [mm]
L – axial distance from the nozzle lip, [mm]
L_c – collar length, [mm]
L_p – straight pipe length, [mm]
r – radial distance from the nozzle axis, [mm]
Re – Reynolds number (= $U_e D/$), [–]
St_e – excitation Strouhal number (= $f_e D/U_e$), [–]
u_c – centerline velocity fluctuation, [m/s]
U_e – centerline exit velocity, [m/s]

References

[1] Hill, W. G. Jr., Greene, P. R., Increased Turbulent Jet Mixing Rates Obtained by Self-Excited Acoustic Oscillations, Trans. ASME: *Journal of Fluids Engineering, 99* (1977), pp. 520-525

[2] Crow, S. C., Champagne, F. H., Orderly Structure in Jet Turbulence, *J. Fluid Mech., 48* (1971), part 3, pp. 547-591

[3] Hasan, M. A. Z., Hussain, A. K. M. F., A Formula for Resonance Frequencies of a Whistler Nozzle, *Journal of the Acoustical Society of America, 65* (1979), 5, pp. 1140-1142

[4] Seol, W. S., Goldstein, R. J., Visualization of the Effect of Acoustic Excitation on Vortex Structure and Energy Separation in Jets, *Proceedings,* 11th International Heat Transfer Conference, Kyongju, Korea, 1998, vol. 5, pp. 491-496

[5] Brown, G. B., Roshko, A., On Density Effect and Large Structure in Turbulent Mixing Layers, *J. Fluid Mech., 64* (1974), pp. 775-816

[6] Ho, C.-M., Nosseir, N. S., Dynamics of an Impinging Jet. Part 1, The Feedback Phenomenon, *J. Fluid Mech., 105* (1981), pp. 119-142

[7] Yule, A. J., Large-Scale Structure in the Mixing Layer of a Round Jet, *J. Fluid Mech., 89* (1978), part 3, pp. 413-432

[8] Cvetinović, D. B., Ukai, M., Nakabe, K. Suzuki, K., Visualizations on Flow Structures of a Self-Sustained Oscillating Jet and Its Enhanced Region of Impingement Heat Transfer, 9th International Symposium on Flow Visualization, Edinburgh, GB, 2000, pp. 70-1 – 70-7

[9] Cvetinović, D., Tihon, J., Verjazka, J., Drahos, J., Effect of External Excitations on the Axisymmetrical Air Jet Flow Structures – Investigations of the Free Jet, *Proceedings on CD*, CHISA 2004, Prague, Czech Republic, Paper No. 5.237

Authors' addresses:

D. Cvetinović
VINČA Institute of Nuclear Science
Laboratory for Thermal Engineering and Energy,
P. O. Box 522, 11001 Belgrade, Serbia

M. Ukai[1], K. Nakabe[2], and K. Suzuki[3]
Department of Mechanical Engineering, Heat Transfer Laboratory,
Kyoto University,
Kyoto 606-8501, Japan

Present authors' addresses:
[1] Osaka gas Co., LTD.
    Engineering Department, Process Engineering Team
    Osaka, Japan

[2] Osaka Prefecture University
    Department of Mechanical Engineering, Applied Energy Science Laboratory,
    Sakai, Osaka 599-8531, Japan

[3] Shibaura Institute of Technology
    Mechanical Control Systems Department
    307 Fukasaku, Saitama 337-8570, Japan

Corresponding author (D. Cvetinović):
E-mail: deki@vin.bg.ac.yu